First publ. in: Organometallics 11 (1992), pp. 3894–3900

Electronic Structure of Triple-Decker Sandwich Complexes with P_6 Middle Rings. Synthesis and X-ray Structure Determination of Bis(η^5-1,3-di-*tert*-butylcyclopentadienyl)-(μ-η^6:η^6-hexaphosphorin)diniobium

A. Chandrasekhar Reddy and Eluvathingal D. Jemmis*

School of Chemistry, University of Hyderabad, Central University, P.O., Hyderabad—500 134, India

Otto J. Scherer,* Rainer Winter, Gert Heckmann,† and Gotthelf Wolmershäuser†

Fachbereich Chemie der Universität Kaiserslautern, Erwin-Schrödinger-Strasse, D-6750 Kaiserslautern, Germany

Received June 10, 1992

The cothermolysis of [Cp″Nb(CO)$_4$] (1), Cp″ = $C_5H_3(^tBu)_2$-1,3, and P_4 affords the 26-valence-electron triple-decker sandwich complex [(Cp″Nb)$_2$(μ-η^6:η^6-P_6)] (2). Its X-ray structure determination shows that the P_6 middle deck is severely bisallylically distorted (orange crystals, monoclinic space group $P2_1/n$, a = 10.139 (1) Å, b = 12.206 (1) Å, c = 13.477 (1) Å, β = 108.64 (1)°, V = 1580.4 Å^3, Z = 2, R = 0.0359, R_w = 0.0478). Extended Hückel calculations have been carried out to explain the distortion in this and several other triple-decker complexes with P_6 middle decks. The in-plane distortion of the cyclo-P_6 ligand observed in 26-valence-electron (VE) triple-decker complexes is traced to the presence of two electrons in the nearly degenerate $2e_2'$ antibonding orbitals. In 24-VE systems the strong interaction between the metal–metal bonding orbital, a_2'', and the top most π^*-orbital of the puckered P_6 ring is responsible for the puckering of the P_6 ring. Additionally this type of distortion is favored by a decrease of energy of the $1e_2'$ orbitals and the larger HOMO–LUMO gap. In comparison to P_6 and As_6 the C_6H_6 ligand is far less susceptible to such an out of plane distortion because the high lying b_{2g} orbital provides only a small interaction with the metal–metal bonding orbital. The 24-VE triple-decker complexes may gain extra stability by three-dimensional delocalization depending on the type of middle ring present in the complex.

Introduction

During the last six years many novel triple-decker sandwich complexes with cyclo-P_n—or cyclo-As_n—units as middle deck have been synthesized.[1a,b] Several theoretical studies gave some insight into the bonding and electronic structure of these compounds.[2,3]

All the triple-decker complexes with P_6 middle rings that have been examined by X-ray structure analyses are collected in Table I.

A closer examination reveals a relationship between the electron count and the structure present in these compounds. Complexes with 28 valence electrons (VE) (M = Mo, W) have undistorted, symmetric, and planar middle rings. Decreasing the VE count from 28 to 26 or 24 provides two different types of distortions of the middle rings.

In the 26-VE triple-decker complexes of group 5 metals (M = V, Nb) an in-plane distortion of the P_6 ligand is observed. In the Nb complex [(Cp′Nb)$_2$(μ-η^6:η^6-P_6)][6] four short and two long P–P bonds are found, whereas the opposite situation is found in the V complex.[5]

In all complexes with electron counts ranging from 28 to 26 the P_6 middle ring is planar. Since the HOMOs, 5 (cf. Figures 2 and 5), are antibonding between the metals and the middle ring in 28-VE systems, the bonding should increase as four electrons are removed from these orbitals. Unexpectedly, the P_6 ligand in the 24-VE complex [(Cp*Ti)$_2$(μ-η^3:η^3-P_6)][7] is puckered.

In the present paper we present the synthesis, the spectroscopic and structural characterization, and the electronic structure of the 26-VE triple-decker sandwich compound [(Cp″Nb)$_2$(μ-η^6:η^6-P_6)] (2). We further study the distortions of the P_6 middle rings in the complexes mentioned above as a function of the number of valence electrons.

Table I. Crystallographically Characterized Triple-Decker Complexes with P_6 Middle Rings and the Number of Valence Electrons Present in Them

complex[a]	no. of valence electrons (VE)	ref
[(Cp*Mo)$_2$(μ-η^6:η^6-P_6)]	28	4
[(Cp*W)$_2$(μ-η^6:η^6-P_6)]	28	5
[(Cp′V)$_2$(μ-η^6:η^6-P_6)]	26	5
[(Cp′Nb)$_2$(μ-η^6:η^6-P_6)]	26	6
[(Cp″Nb)$_2$(μ-η^6:η^6-P_6)]	26	this work
[(Cp*Ti)$_2$(μ-η^3:η^3-P_6)]	24	7

[a] Cp* = η^5 – C_5Me_5; Cp′ = η^5 – C_5Me_4Et; Cp″ = $C_5H_3(^tBu)_2$-1,3.

Experimental Section

General Procedures. All manipulations were performed under an argon atmosphere by using standard Schlenk techniques. Toluene, decalin, *n*-hexane, and light petroleum benzene were dried and distilled from Na or Na/K alloy under argon. Bu_3SnCl was purchased from Merck and distilled under argon prior to use.

* Authors to whom correspondence should be addressed.
† X-ray structure analysis.

(1) (a) Scherer, O. J. *Angew. Chem.* **1990**, *102*, 1137; *Angew. Chem., Int. Ed. Engl.* **1990**, *29*, 1104. (b) Scheer, M.; Herrmann, E. *Z. Chem.* **1990**, *30*, 41.
(2) Jemmis, E. D.; Reddy, A. C. *Organometallics* **1988**, *7*, 1561.
(3) Tremel, W.; Hoffmann, R.; Kertesz, M. *J. Am. Chem. Soc.* **1989**, *111*, 2030.
(4) Scherer, O. J.; Sitzmann, H.; Wolmershäuser, G. *Angew. Chem.* **1985**, *97*, 358; *Angew. Chem., Int. Ed. Engl.* **1985**, *24*, 351.
(5) Scherer, O. J.; Schwalb, J.; Swarowsky, H.; Wolmershäuser, G.; Kaim, W.; Gross, R. *Chem. Ber.* **1988**, *21*, 443.
(6) Scherer, O. J.; Vondung, J.; Wolmershäuser, G. *Angew. Chem.* **1989**, *101*, 1359; *Angew. Chem., Int. Ed. Engl.* **1989**, *28*, 1355.
(7) Scherer, O. J.; Swarowsky, H.; Wolmershäuser, G.; Kaim, W.; Kohlmann, S. *Angew. Chem.* **1987**, *99*, 1178; *Angew. Chem., Int. Ed. Engl.* **1987**, *26*, 1153.

BuLi was used as obtained from Aldrich. Cp″ (Cp″ = C_5H_3-($^tBu_2$)-1,3) was prepared as described in literature.[8,9] White phosphorus was obtained from Merck and dried in vacuo before use. $NbCl_5$ (Ventron) was sublimed twice and used immediately after. Column chromatography was carried out under an atmosphere of argon on silica gel (Macherey–Nagel, 0.06–0.2 mm), which was heated at 180 °C for 20 h, deactivated with 3% of degassed water, and stored under argon.

C, H, and N analyses were performed at the University of Kaiserslautern on a Perkin-Elmer 2400 CHN analyzer. NMR spectra were recorded on a Bruker WP 200 or a Bruker AM 400 spectrometer at ambient temperatures in C_6D_6 as solvent. Residual C_6D_5H was taken as internal standard; coupling constants are given in hertz. Infrared spectra were run on a Perkin-Elmer 881 infrared spectrophotometer. The recording of UV/vis data was performed on a Varian CARY 2200. Mass spectra were obtained on a Finnigan MAT 90 instrument using the heated probe for volatilization and EI for ionization of the sample. Only the most characteristic fragments are reported.

Preparation of the Complexes and Spectroscopic Data. Cp″Sn(nBu)$_3$. This compound was synthesized according to a method reported for Cp*Sn(nBu)$_3$ (Cp* = C_5Me_5).[10] Cp″H (41.1 g, 0.23 mmol) was dissolved in 800 mL of THF; 155 mL of BuLi (1.6 M in *n*-hexane, 0.25 mmol) was added through a dropping funnel over 2 h, and the resulting bright orange solution was stirred until the evolution of butane had ceased. Then 81.4 g of Bu_3SnCl (0.25 mmol) was added over 30 min through a dropping funnel and left under stirring overnight. The solvent was then removed on a rotary evaporator. To the resulting thick yellow oil was added 60 mL of hexane, which caused the LiCl to precipitate. This was removed by centrifugation at about 3000 rpm and then extracted with another 40 mL of *n*-hexane. Hexane was pumped off in vacuo from the combined solutions and the resulting yellow oil distilled in vacuo. Cp″Sn(nBu)$_3$ was obtained as a bright yellow oil at 156–159 °C and purified by distillation over a 12 cm vigreux column (86.1 g, 0.184 mmol; overall yield, 79.8%). Cp″Sn(nBu)$_3$ is stable under inert gas atmosphere and can be stored for long periods at ambient temperature without decomposition: ^{1}H NMR (C_6D_6), 298 K) δ 6.39 [t, 1 H, ^4J(H–H) = 1.1, ^4J(Sn–H) = 12.6], 4.89 [d, 2 H, ^4J(H–H) = 1.1, ^2J(Sn–H) = 36.5], 1.45 [m, 6 H], 1.30 [m, 6 H], 1.20 [s, 18 H], 0.90 [t, 9 H, ^3J(H–H) = 7.3], 0.82 [t, 6 H, ^3J(H–H) = 8.3]; ^{13}C NMR (C_6D_6, 298 K) δ 154.3 [s], 121.6 [d, J(C–H) = 157, ^3J(Sn–C) = 22], 84.0 [d, J(C–H) = 150, J(Sn–C) = 36], 32.8 [s], 31.8 [q, J(C–H) = 125], 29.5 [t, J(C–H) = 122, ^2J(Sn–C) = 19], 27.8 [t, J(C–H) = 122, ^3J(Sn–C) = 61], 13.9 [q, J (C–H) = 125, ^4J(Sn–C) = 24], 12.3 [t, J(C–H) = 127, J(Sn–C) = 310]; ^{117}Sn NMR (C_6D_6, 298 K, $SnMe_4$, ext) δ –20.4 [m]; IR (film, cm^{-1}) 2959 (s), 2930 (s), 2871 (s), 2860 (s), 1670 (w), 1574 (w), 1464 (m), 1418 (w), 1389 (m), 1378 (m), 1359 (m), 1292 (w), 1259 (m), 1246 (m), 1119 (m), 1074 (m), 1025 (m), 1004 (m), 960 (w), 925 (w), 881 (m), 839 (m), 810 (w), 780 (w), 662 (m). MS (EI, 20 eV, 298 K), m/z (fragment, rel intensity), (all Sn-containing peaks show the Sn isotopic pattern, rel intensities are based on ^{120}Sn, R = C_4H_9, X = Cp″) 468 (M^+, 4), 411 M^+ – R, 8), 291 (M^+ – X, 100), 269 ($C_{11}H_{49}Sn$, 66), 235 (R_2SnH^+, 59), 177 (RSn^+, 22), 57 (R^+, 8). Anal. Found (Calcd for $C_{25}H_{48}Sn$): C, 64.21 (64.25); H, 10.33 (10.35).

[Cp″Nb(CO)$_4$] (1). The synthesis of [Cp″Nb(CO)$_4$] was carried out as described for [Cp*Nb(CO)$_4$].[10] In a typical run $NbCl_5$ (11.73 g, 43.4 mmol) were suspended in 1100 mL of dry toluene and stirred overnight. The resulting bright orange-red suspension was heated under reflux until all the $NbCl_5$ had dissolved. The heating has removed and an equimolar amount of Cp″Sn(nBu)$_3$ (20.28 g) added through a syringe in three portions to the hot solution. Immediately after addition the color of the solution intensified to deep red. The solution was allowed to cool to room temperature during 60 min while stirring was continued. The solvent was then distilled off in vacuo, and the resulting, deep red oily residue was extracted several times with dry petroleum benzene to remove the Bu_3SnCl formed in the reaction. The resulting red tarry residue was first dried in vacuo and then dissolved in 250 mL of freshly distilled THF ([Cp″$NbCl_4$] is highly susceptible to moisture). Finely ground Zn powder (7.9/g), Al bronze (2.3 g) and Cu powder (4.5 g) were degassed in vacuo and added to the dark red solution. The whole mixture was transferred under inert gas in a 500-mL turning autoclave. The system was closed and CO added until a pressure of about 250 bar was reached. The autoclave was rotated for 60 min. When the solution was saturated with CO a pressure of about 230 bar remained. The autoclave was then heated to 100–105 °C mantle temperature which caused the internal pressure to reach 290–295 bar. These conditions were applied for 120 h. After cooling to ambient temperature and removal of the CO gas the reddish brown suspension was filtered over a 5-cm layer of silica gel. The solvent was evaporated in vacuo and the resulting powdery residue loaded on a silica gel column (30 × 2.5 cm, water cooled). Chromatography with petroleum benzene as eluent gave an orange red band of 1. Evaporation of the solvent left an intense red oily residue which solidified after cooling in a refrigerator for several days. This material contains some impurities (mainly solvent and Bu_3SnCl) but can be used without further purification for the following experiments after ^{1}H NMR spectroscopic determination of the [Cp″Nb(CO)$_4$] content. The analytically pure material can be obtained by repeated sublimation of the crude product: yield 2.18 g of the purified material (5.7 mmol, 13.7%). ^{1}H NMR (C_6D_6, 298 K) δ 5.30 [m, br, 1 H], 4.91 [m, br, 2 H], 0.96 [s, 18 H]; ^{13}C NMR (C_6D_6, 298 K) δ 156.6 [s], 155.8 [s], 139.3 [s], 138.9[s], 133.0 [s], 90.3 [d, J(C–H) = 170], 90.1 [d, J(C–H) = 167], 32.1 [q, J(C–H) = 126], 31.5 [s]; ^{93}Nb NMR (C_6D_6, 298 K, $NbCl_5$, ext) –2170 [s]; IR (KBr, cm^{-1}); 2907 (m), 2869 (m), 2022 (s), 1910 (vs, br), 1609 (w, br), 1461 (m), 1391 (m), 1370 (m), 1362 (m), 1256 (m), 1198 (w), 1053 (m), 1025 (m), 922 (w), 837 (w), 798 (m), 665 (m). Anal. Found (Calcd for $C_{17}H_{21}NbO_4$): C, 53.78 (53.42); H, 5.73 (5.54).

[(Cp″Nb)$_2$(μ-η^6:η^6-P$_6$)] (2). 1 (0.38 g, 1 mmol) and vacuum dried P_4 (0.48 g, 3.9 mmol) were dissolved in 50 mL of dry decalin and the solution then heated under magnetic stirring to 165–168 °C. Monitoring the reaction by means of IR spectroscopy revealed a steady decrease of the intensity of the absorption bands of the educt. Heating was stopped after ca. 120 min when no more absorption in the carbonyl region was detected. After cooling, the solvent and unreacted phosphorus were removed by distillation/sublimation. The oily brownish residue was dissolved in 3 mL of CH_2Cl_2, 3 g of silica gel was added, and the solution was evaporated until free flowing. This mixture was loaded on a silica gel column (30 × 2 cm, water cooled). Petroleum benzene gave an orange fraction of **2**, which was concentrated to ca. 10 mL and kept at 5 °C for 3 days. [(Cp″Nb)$_2$(μ-η^6:η^6-P$_6$)] could then be collected as orange crystals. Another crop could be obtained by further concentration of the mother liquor to about 3 mL and cooling for several days. The crystals were washed with cold pentane and dried in vacuo: total yield 168 mg (0.23 mmol, 23.2%); ^{1}H NMR (C_6D_6, 298 K) δ 4.46 [t, 2 H, ^4J(H–H) = 2.2], 4.36 [d, 4 H, ^4J(H–H) = 2.2], 1.02 [s, 36 H]; ^{13}C NMR (C_6D_6, 298 K) δ 131.8 [s], 91.6 [d, J(C–H) = 172], 90.1 [d, J(C–H) = 169], 32.2 [s], 31.7 [q, J(C–H) = 126]; ^{31}P NMR (C_6D_6, 298 K) δ 115 [s]; ^{93}Nb NMR (C_6D_6, 298 K, $NbCl_5$, ext) δ 626 (very broad); IR (KBr, cm^{-1}) 2955 (s), 2910 (m), 2899 (m), 2862 (m), 1633 (m, br), 1486 (m), 1461 (m), 1391 (m), 1367 (m), 1357 (m), 1289 (w), 1259 (m), 1249 (m), 1195 (w), 1162 (m), 1095 (m), 1051 (m), 1022 (m), 935 (w), 918 (w), 834 (s), 811 (m), 799 (s), 665 (m); MS (EI, 70 eV, 190 °C) m/z (fragment, rel intensity) 726 (M^+, 45), 654 (M^+ – C_5H_{12}, 7), 612 (M^+ – 2 × C_4H_9, 4), 363 (M^{2+}, 4), 124 (P_4^+, 9), 57 ($C_4H_9^+$, 100), 44 ($C_3H_8^+$, 81); UV/vis (CH_2Cl_2), λ_{max} (nm), [ϵ(cm^2 mol^{-1})] 497 [700], 440 [865], 407 [1005], 358 [1900]. Anal. Found (Calcd for $C_{26}H_{42}Nb_2P_6$): C, 43.06 (43.00); H, 5.85 (5.83). Petroleum benzene/toluene (10:1) gave an additional green fraction. Evaporation of the solvent yielded 36 mg of a substance with the composition [(Cp″Nb)$_3$P$_6$] (**3**) (0.036 mmol, 3.6%) which demands no further discussion in this context.

Crystallographic Analysis for 2. Crystallographic data are collected in Table II. X-ray study was carried out by using an Enraf–Nonius CAD 4 diffractometer. Intensity data were obtained by variable-rate $\Omega - {}^2/_3\Theta$ scans with Mo Kα radiation (λ = 0.71069 Å, graphite monochromator). A total of 2744 unique reflections were collected in the range 1.50° ≤ Θ ≤ 25° with 2270 reflections having $I \geq 2\sigma(I)$. Lattice parameters were obtained by a least-squares analysis of 25 reflections in the range 20.33° ≤ Θ ≤ 24.0°

(8) Riemschneider, R.; Nehring, R. *Monatsh. Chem.* **1959**, *90*, 568.
(9) Riemschneider, R. *Z. Naturforsch.* **1963**, *18b*, 641.
(10) Herrmann, W. A.; Kalcher, W.; Biersack, H.; Bernal, I.; Creswick, M. *Chem. Ber.* **1981**, *114*, 3558.

Table II. Data for the X-ray Diffraction Analysis of 2

formula	$C_{26}H_{42}Nb_2P_6$
mol mass g/mol	726.28
space group	$P2_1/n$, monoclinic
a, Å	10.139 (1)
b, Å	12.206 (1)
c, Å	13.477 (1)
β, deg	108.64 (1)
Z	2
V, Å^3	1580.4 (2)
ρ(calcd), g/cm^3	1.526
color	orange
T, K	298
cryst dimens, mm	0.3 × 0.4 × 0.25
no. of unique data	2744
no. of obsd data	2270 ($2\sigma(I)$ criterion)
R	0.0359
R_w	0.0478

Table III. Selected Bond Distances (Å) and Angles (deg) for [(Cp″Nb)$_2$(μ-η^6:η^6-P$_6$)] (2)

Bond Distances			
P(1)–P(2)	2.347 (3)	P(2)–P(3)	2.116 (3)
P(1)–P(3′)	2.105 (2)	Nb–Nb′	2.828 (1)
P(1)–Nb	2.591 (2)	P(1′)–Nb	2.546 (2)
P(2)–Nb	2.531 (1)	P(2′)–Nb	2.575 (2)
P(3)–Nb	2.719 (1)	P(3′)–Nb	2.678 (1)
C(1)–Nb	2.459 (5)	C(2)–Nb	2.436 (5)
C(3)–Nb	2.449 (5)	C(4)–Nb	2.403 (5)
C(5)–Nb	2.409 (5)		
Nb–P$_{6(centroid)}$	1.414 (1)	Nb–Cp″$_{(centroid)}$	2.113 (5)

Bond Angles			
P(1)–P(2)–P(3)	122.6 (1)	P(2)–P(3)–P(1′)	115.4 (1)
P(3′)–P(1)–P(2)	121.7 (1)		
P(1)–Nb–P(2)	54.5 (1)	P(1′)–Nb–P(2′)	54.6 (1)
P(2)–Nb–P(3)	47.4 (1)	P(2′)–Nb–P(3′)	47.5 (1)
P(3)–Nb–P(1′)	47.0 (1)	P(3′)–Nb–P(1)	47.0 (1)
Nb–P(1)–Nb′	66.8 (1)	Nb–P(2)–Nb′	67.3 (1)
Nb–P(3)–Nb′	63.2 (1)		
Cp″$_{(centroid)}$–Nb–P$_{6,centr}$	178.5	Nb–P$_{6(centroid)}$–Nb′	180.0

scattered in reciprocal space, obtained from the automatic centering routine. Intensities of three standard reflections were monitored after every 2 h. The solution and refinement of the structure were performed on a Siemens 7.551 computer using SHELX-76 and SHELXS-86 packages. The atomic scattering factors were taken from ref 11. The data were corrected for Lorentz and polarization effects. The structure was solved by direct methods and refined by standard least-squares and difference Fourier methods. The function minimized was $\omega(F_o - F_c)^2$ with the weights, ω, assigned as $1/[\sigma^2 F_o + (2 \times 10^{-4})F_o^2]$. Hydrogen atoms were placed on the calculated positions and not refined. A common temperature factor was given to equivalent H atoms. The highest peak in the final difference Fourier map had a height of 0.58 e/Å^3.

Results and Discussion

Molecular Structure of [(Cp″Nb)$_2$(μ-η^6:η^6-P$_6$)] (2). The cothermolysis of [Cp″Nb(CO)$_4$] (1) and P$_4$ affords the triple-decker sandwich complex **2** and the trinuclear compound **3**[12] (Scheme I).

Scheme I

$$[\underset{\mathbf{1}}{Cp''Nb(CO)_4}] + P_4 \xrightarrow[165\text{–}168\ ^\circ C]{\text{decalin}} [\underset{\mathbf{2}}{(Cp''Nb)_2(\mu\text{-}\eta^6\text{:}\eta^6\text{-}P_6)}] + [\underset{\mathbf{3}}{(Cp''Nb)_3P_6}]$$

$$Cp'' = C_5H_3(^tBu)_2\text{-}1,3$$

Complex **2** forms orange crystals which are briefly stable in air, moderately soluble in pentane, and readily to very readily soluble in toluene and dichloromethane. The structure of **2** has been unambiguously established by X-ray crystallography (Figure 1).

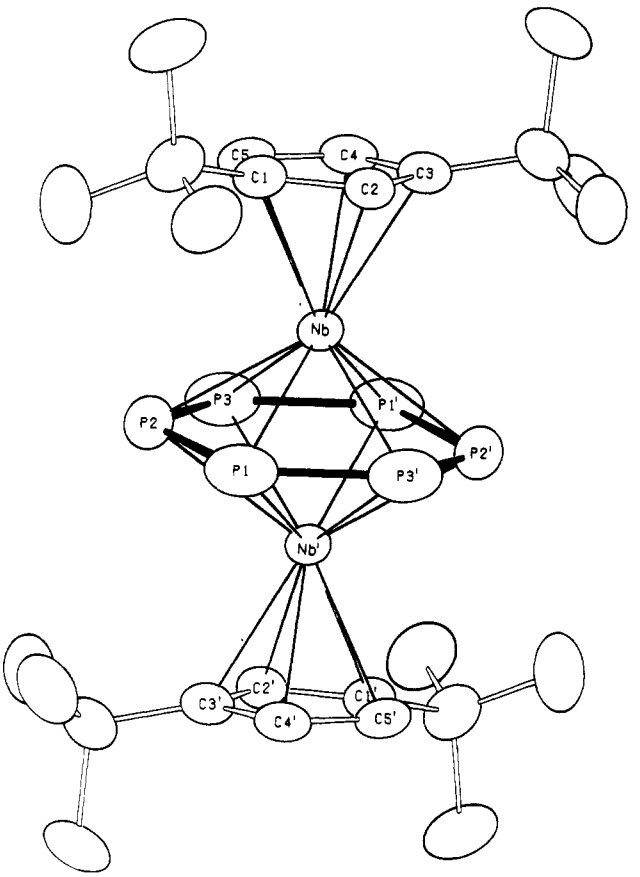

Figure 1. Crystal structure of the 26-VE triple-decker sandwich complex [(Cp″Nb)$_2$(μ-η^6:η^6-P$_6$)] (**2**). Thermal ellipsoids are represented at 50% probability.

The three decks are essentially planar and parallel to each others with a Nb–P$_{6(center)}$–Nb′ angle of 180.0 and a Cp″$_{(center)}$–Nb–P$_{6(center)}$ angle of 178.5°, respectively (Table III). The metal centers are located unsymmetrically between the two decks with a Nb–P$_{6(center)}$ distance of 1.41 Å, which is much shorter than the Nb–Cp″$_{(center)}$ distance of 2.11 Å. The Cp″ ligands are rotated with respect to each other by 180°, which produces an inversion center located in the middle of the P$_6$ ring.

The most striking feature, however, is the severe bisallylic distortion of the six-membered phosphorus middle deck. Two pairs of short P–P bonds, P1–P3′ and P1′–P3 with a bond length of 2.105 (2) Å and P2–P3 and P2′–P3′ with a bond length of 2.116 (3) Å, average at 2.11 Å, a value about 0.24 Å shorter than the long P1–P2 and P1′–P2′ bonds of 2.347 (3) Å. Furthermore, this distortion divides the P–P–P, P–Nb–P$_{neighbor}$, and the Nb–P–Nb′ angles into two sets of acute and obtuse angles.

As for the P–P–P angles, those at a P atom of the long P–P bonds (P1, P1′, P2, P2′) are larger than 120° (122.6 (1)° and 121.7 (1)°), whereas the other ones are acute (115.4 (1)°). Similar conditions are found for the Nb–P–Nb′ angles (Nb–P1–Nb′ = 66.8 (1)°, Nb–P2–Nb′ = 67.3 (1)°, Nb–P3–Nb′ = 63.2 (1)°). On the other hand, those P–Nb–P$_{neighbor}$ angles, where both P atoms belong to the short P–P bonds are much smaller (47.0 (1)° to 47.5 (1)°) than the remaining two (54.5 (1)° and 54.6 (1)°).

Whereas triple-decker sandwich complexes of group 6 metals with an electron count of 28 VE do not exhibit any distortion of the middle P$_6$ ring at all,[1a] a slight distortion is a general phenomenon for all comparable compounds

(11) *International Tables for X-ray Crystallography*; Kynoch Press: Birmingham, England, 1974; Vol. IV (present distributor: Kluwer Academic Publishers, Dordrecht).
(12) Scherer, O. J.; Winter, R. Unpublished results.

Table IV. Selected Structural Data for Group 5 Triple-Decker Complexes $[(M)_2(\mu\text{-}\eta^6\text{:}\eta^6\text{-}P_6)]$ with a P_6 Ring as Middle Deck with Respect to Its Bisallylic Distortion

	d_{P-P}, Å			d_{M-P}, Å			$\angle_{P-M-P}$, deg			$\angle_{M-P-M}$, deg			
(M)	l[a]	s[b]	Δ[c]	l[a]	s[b]	Δ[c]	l[a]	s[b]	Δ[c]	l[a]	s[b]	Δ[c]	ref
Cp′V	2.151*	2.097	0.054	2.478*	2.518	0.040	51.0*	49.2	1.8	64.1	63.1*	1.0	5
Cp′Nb	2.242	2.157*	0.085	2.577	2.624*	0.047	51.6	49.0*	2.6	65.6*	64.3	1.3	6
Cp″Nb	2.347	2.111*	0.236	2.561	2.699*	0.138	54.6	47.3*	7.3	67.1*	63.2	3.9	*d*

[a] l = long P–P edge. [b] s = short P–P edge. [c] Δ = difference between long and short edges. *average value, Cp′ = η^5-C_5Me_4Et, Cp″ = η^5-$C_5H_3(^tBu)_2$-1,3. [d] This work.

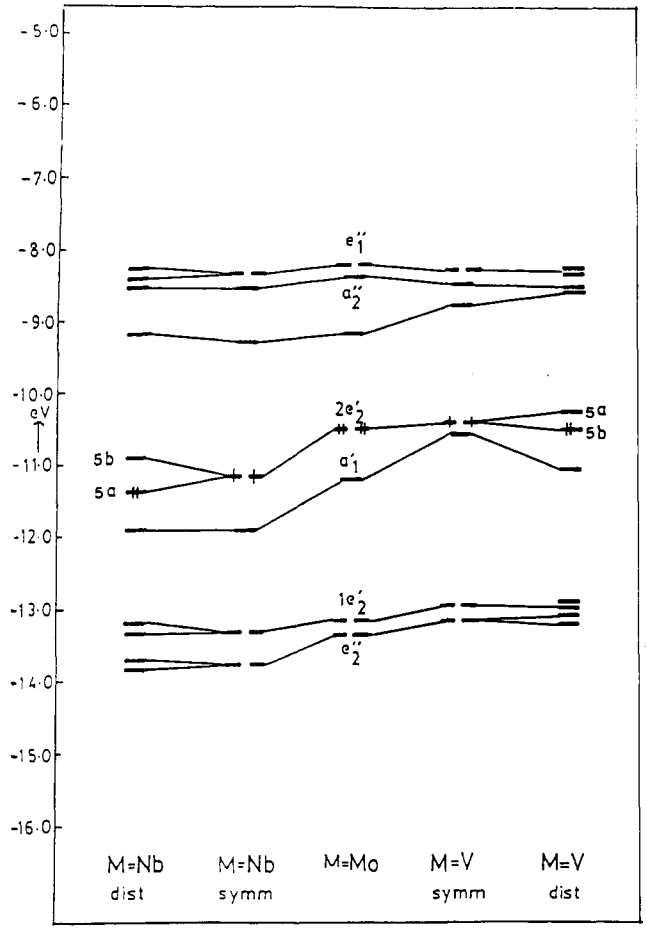

Figure 2. Correlation of the energy levels of triple-decker sandwich compounds of the type $[CpMP_6MCp]$ (M = Nb, Mo, V).

of group 5 metals with two VE less. But in none of these compounds is this distortion as severe as it is in **2**. This is evidenced by the comparison of the relevant structural data of all characterized compounds in question, given in Table IV.

It is worthwhile to mention that in the 26-VE triple-decker sandwich complex $[(CpV)_2(\mu\text{-}\eta^6\text{:}\eta^6\text{-}C_6H_6)]$ X-ray crystallographically a separation of the benzene π system into two allyl-like $3e^-$ units was found.[13] The complex $[(Cp'V)_2(\mu\text{-}\eta^6\text{:}\eta^6\text{-}P_6)]$ with the same electron count has a distorted P_6 unit; here, however, the distortion leads to two short and four long P–P bonds.[5]

Electronic Electronic Structure of $[CpMP_6MCp]$ (M = V, Nb) and the in-Plane Distortion of the P_6 Ring. EHMO calculations on the 28-VE complex $[CpMoP_6MoCp]$ revealed[2,3] that the degenerate HOMOs, $2e_2'$, (Figure 2, middle) are antibonding between the middle ring and the metal fragments, **5**.

In 28-VE systems **5a** and **5b** are both filled, and a symmetric triple-decker complex is obtained. In 26-VE complexes $[CpMP_6MCp]$ (M = V, Nb), however, the nearly

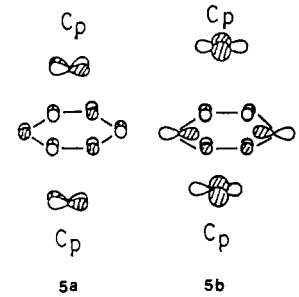

5a **5b**

degenerate HOMOs, **5**, are only half filled. On the right and left side of Figure 2 Walsh diagrams for the in-plane distortion of the P_6 ring in the V and Nb complexes are given.

Going from a symmetric planar to a distorted planar P_6 ring leaves the e_2'', $1e_2'$, and a_1' levels almost unchanged in energy but induces a significant splitting of the $2e_2'$ orbitals into the two components **5a** and **5b**.

Up to now two crystallographically characterized 26-VE complexes of the type under discussion have appeared in literature. In the V complex $[(Cp'V)_2(\mu\text{-}\eta^6\text{:}\eta^6\text{-}P_6)]$,[5] two short and four long P–P bonds are observed, whereas the Nb complexes $[(Cp'Nb)_2(\mu\text{-}\eta^6\text{:}\eta^6\text{-}P_6)]$[6] and $[(Cp''Nb)_2(\mu\text{-}\eta^6\text{:}\eta^6\text{-}P_6)]$ (**2**) reported herein show the opposite bisallylic distortion (four short and two long P–P bonds). These two different modes of in-plane distortion correspond to the occupancy of either **5a** or **5b**. It is, however, difficult to specify which factors control the type and amount of in-plane distortions found in 26-VE complexes with P_6 as middle ring.

A similar type of bisallylic distortion is observed in the triple-decker complex $[(CpV)_2(\mu\text{-}\eta^6\text{:}\eta^6\text{-}C_6H_6)]$ with the same electron count.[13] Calculations on this compound[2,14] showed that the factors responsible for the bisallylic distortion of the C_6H_6 middle ring are very much the same as in the P_6 middle ring systems.

Electronic Structure of $[CpTiP_6TiCp]$ with Planar (4a) and Puckered P_6 Rings (4b). In order to get insight into the puckering of the P_6 ring observed in the 24-VE complex $[(Cp^*Ti)_2(\mu\text{-}\eta^3\text{:}\eta^3\text{-}P_6)]$[7] we calculated the interaction between CpTi···TiCp and planar as well as puckered P_6-ring fragments. In Figure 3a the orbitals of $[CpTiP_6TiCp]$ with a planar P_6 ring are depicted. The electronic structure of this complex resembles the electronic structure of any metal–metal bonded triple-decker

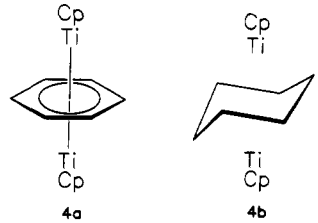

4a **4b**

(13) Angermund, K.; Claus, K. H.; Goddard, R.; Krüger, C. *Angew. Chem.* **1985**, *97*, 241; *Angew. Chem., Int. Ed. Engl.* **1985**, *24*, 237.

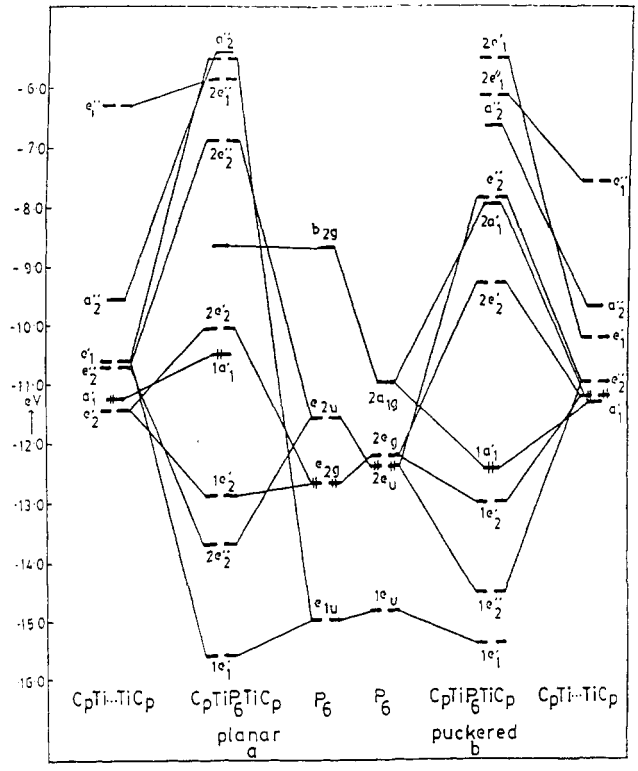

Figure 3. Construction of the orbitals of [CpTiP$_6$TiCp] with planar and puckered P$_6$ rings from the fragments CpTi···TiCp and P$_6$.

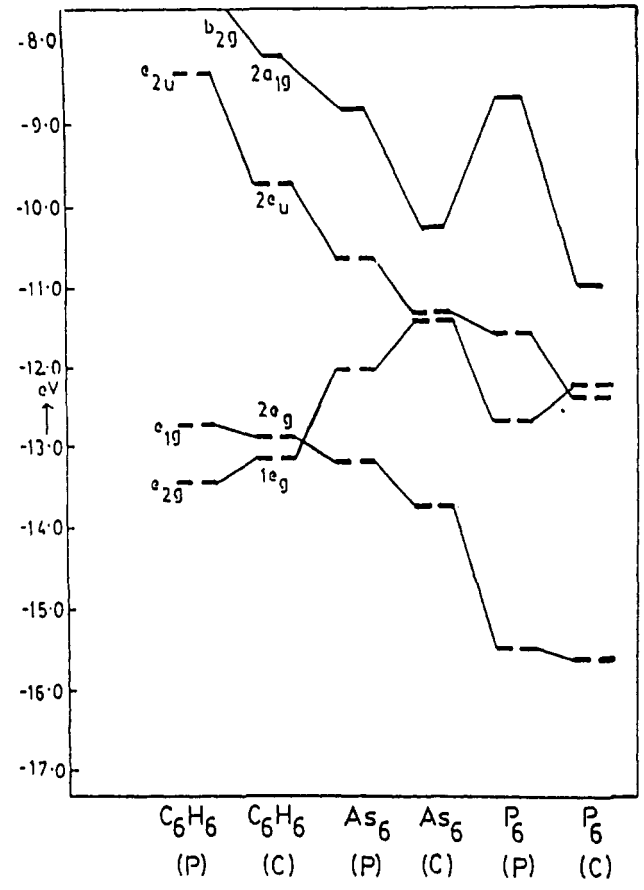

Figure 4. Correlation of the energy levels of C_6H_6, As_6, and P_6 rings in both the planar and the puckered forms. (P) = planar; (C) = puckered.

complex. The important interactions between the CpTi···TiCp and the planar P$_6$ fragment are e_1''/e_{1g}, e_1'/e_{1u}, e_2''/e_{2u}, e_2'/e_{2g}, a_2''/a_{2u}, and a_1'/a_{1g}. (The orbitals of the planar P$_6$ ring are only partially shown in Figure 3.)

In 28-VE systems electrons occupy all orbitals up to the $2e_2'$ level (Figure 3a), which is antibonding between the CpM···MCp fragment and the middle ring. Thus, decreasing the electon count by four electrons to 24 VEs should further stabilize this structure type. Unexpectedly, the 24-VE complex [(Cp*Ti)$_2$(μ-η^3:η^3-P$_6$)] possesses a puckered P$_6$ ring.[7]

To shed light on this phenomenon the orbitals of [CpTiP$_6$TiCp] are constructed from CpTi···TiCp and the puckered P$_6$ fragment. Before we can do so, we first have to consider the changes in orbital energy and symmetry that occur when the planar P$_6$ ring distorts into a puckered conformation. Figure 4 shows the Walsh diagram for P$_6$, As$_6$, and C_6H_6 rings for such a puckering process. D_{6h} symmetry labels are given for the planar ring structures and D_{3d} symmetry labels for the puckered ones. This change in symmetry transforms the b_{2g} and a_{1g} MOs to a_{1g}, the e_{1u} and e_{2u} MOs to e_u, the e_{1g} and e_{2g} MOs to e_g, and a_{2u} and b_{1u} to a_{2u} symmetry (cf. Figure 3).

As the planar P$_6$ ring distorts to a puckered P$_6$-ring structure, the energies of the former b_{2g}, e_{1g}, and e_{2u} orbitals decrease significantly, and there is a smaller increase of the energy of the former e_{2g} orbitals. The effect of puckering on the energies of the remaining orbitals is almost negligible.

In D_{6h} symmetry there are no two sets of orbitals with the same symmetry labels and each orbital of the planar P$_6$ ring interacts independently with an orbital of the CpTi···TiCp fragment of appropriate energy and symmetry.

In the puckered P$_6$ ring structure, however, two sets of orbitals do have the same symmetry; they mix and then interact with the CpTi···TiCp MOs. This interaction is shown in Figure 3b with the CpTi···TiCp MOs on the right and the MOs of the puckered P$_6$ ring on the left side. What are now the decisive differences between the two isomers of [CpTiP$_6$TiCp]?

In the planar form the metal–metal bonding orbital, a_1', is destabilized by the a_{1g} orbital of the P$_6$-ring fragment, **6a**. In the puckered form, however, this orbital is stabilized by interacting with the top most π^* orbital, $2a_{1g}$, of the P$_6$-ring fragment, **6b**.

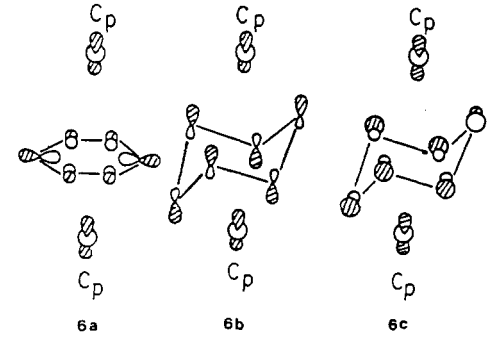

Table V summarizes the fragment overlaps between the CpM···MCp and the P$_6$ middle ring with planar and puckered structures. The fragment overlaps corresponding to the entries a_1'/a_{1g} show that there is an additional contribution to the metal–metal bonding orbital from the a_{1g} orbital, **6c**, of the puckered P$_6$ ring.

Another striking feature is the rise in energy of the e_2' orbitals as the P$_6$ ring distorts to D_{3d} symmetry. The reason for this stronger antibonding interaction is that in the puckered form the $1e_g$ and $2e_g$ orbitals of the P$_6$ ring mix and then interact with the e_2' and e_1'' hybridized or-

Table V. Fragment Overlaps between the Middle-Ring Orbitals and the CpM•••MCp Orbitals

complex[a]		e_1''/e_{1g}	e_1''/e_{2g}	e_2'/e_{2g}	e_2'/e_{1g}	a_1'/a_{1g}	a_1'/b_{2g}
$[CpTiP_6TiCp]$	(P)	0.18		0.14		0.16	
$[CpTiP_6TiCp]$	(C)	0.30	0.13	0.15	0.10	0.23	0.16
$[CpTiAs_6TiCp]$	(P)	0.10		0.16		0.02	
$[CpTiAs_6TiCp]$	(C)	0.21	0.13	0.19	0.03	0.16	0.14
$[CpVP_6VCp]$	(P)	0.14		0.12		0.03	
$[CpVP_6VCp]$	(C)	0.17	0.09	0.14	0.07	0.08	0.15
$[CpTiC_6H_6TiCp]$	(P)	0.42		0.06		0.22	
$[CpTiC_6H_6TiCp]$	(C)	0.40	0.09	0.08	0.09	0.26	0.10
$[CpVC_6H_6VCp]^{2+}$	(P)	0.27		0.06		0.16	
$[CpVC_6H_6VCp]^{2+}$	(C)	0.26	0.05	0.07	0.08	0.16	0.12

[a] (P) = planar, (C) = puckered.

Scheme II

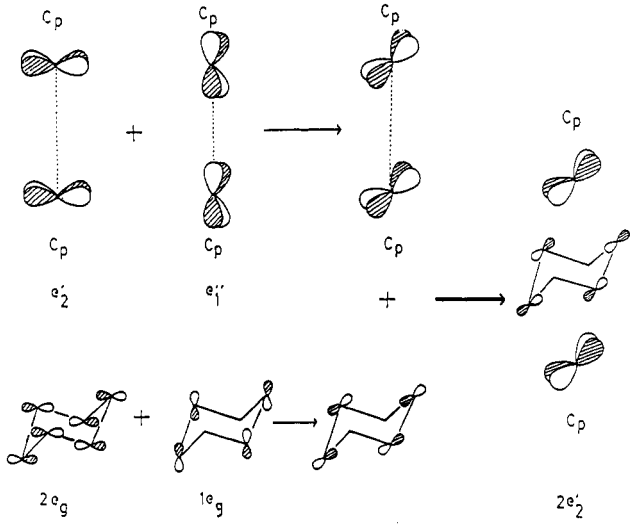

bitals of the CpTi···TiCp fragment (Scheme II), whereas in the planar form the e_2' orbitals of the metal fragment interact with the e_{2g} component of the planar P_6 ring only.

Table V indicates that there is indeed an e_2'/e_{1g} interaction that strengthens the antibonding character of these orbitals. The remaining a_2'', e_1', and e_2'' interactions are almost identical in both, the planar and the puckered structure.

The conclusion to be drawn from the above discussion is that the stabilization of the metal–metal bonding orbital, a_1' (the HOMO in 24-VE complexes), and the destabilization of the $2e_2'$ MOs (which are the LUMOs in these compounds) together control the puckering of the middle ring in 24-VE systems.

As we will discuss later, the puckering in 24-VE complexes depends on both, the metal and the middle ring present in these systems. Figure 5 and a plot of the sum of the one-electron energies as a function of puckering of the middle ring, given in Figure 6, clearly indicate that 24-VE complexes with Ti as the metal and P_6 or As_6 as middle ring should both prefer the puckered structure. Our conclusions are in perfect accordance with the structure observed in $[(Cp^*Ti)_2(\mu\text{-}\eta^3\text{:}\eta^3\text{-}P_6)]$.[7]

If the stabilization of the metal–metal bonding orbital, a_1', is responsible for the puckering of the middle ring in 24-VE systems, what happens then to 26–28-VE systems? In all triple-decker complexes with valence-electron counts from 26 to 28 known to date the middle ring is planar.

These extra two or four electrons enter the $2e_2'$ antibonding MOs which are more antibonding in the puckered structure than in the planar one. This makes the planar triple-decker structure more favorable for both P_6 and As_6 rings as soon as an electron count of 24 is exceeded (Figure 5).

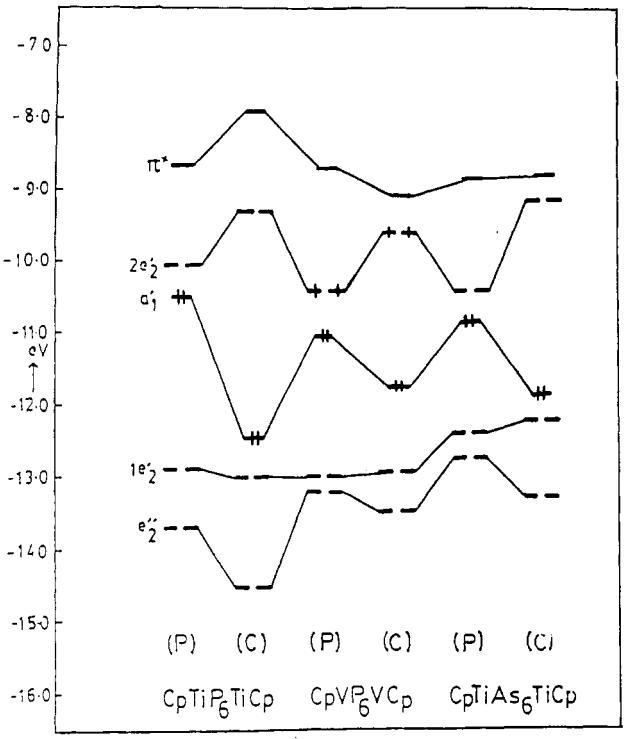

Figure 5. Correlation of the energy levels of $[CpTiP_6TiCp]$, $[CpVP_6VCp]$, and $[CpTiAs_6TiCp]$ in both the planar and the puckered forms. (P) = planar; (C) = puckered.

Puckering of the C_6H_6 Middle Ring in 24-VE Complexes. In order to study the puckering of the C_6H_6 ring, calculations have been carried out on the two 24-VE complexes $[CpTiC_6H_6TiCp]$ and $[CpVC_6H_6VCp]^{2+}$.

According to our calculations the C_6H_6 ring is much less likely to pucker than P_6 or As_6 rings. As we have already discussed the main reason for a puckering of the middle ring is the decrease in energy of the b_{2g} orbital (the top most π^*-orbital) of the C_6H_6 ring. This b_{2g} orbital stabilizes the metal–metal bonding orbital in the puckered form. In the case of P_6 and As_6 rings the energy of the b_{2g} orbital is around −9 eV in the planar form and decreases to −10.5 eV in the puckered structure (Figure 4). The small energy gap between this π^*-orbital of the ring ligand and the metal–metal bonding orbital provides a strong interaction (Figure 3b) and hence stabilizes the metal–metal bonding orbital. In the case of the C_6H_6 ring the energy of the π^*-orbital is −4.75 eV in the planar and −8.20 eV in the puckered structure. This larger energy gap between the π^*-orbital of C_6H_6 in the puckered structure and the metal–metal bonding orbital provides only a weak interaction.

Although the stabilization of the metal–metal bonding orbital is much less in 24-VE C_6H_6 complexes than in P_6 or As_6 systems, $[CpTiC_6H_6TiCp]$ is slightly more stable in

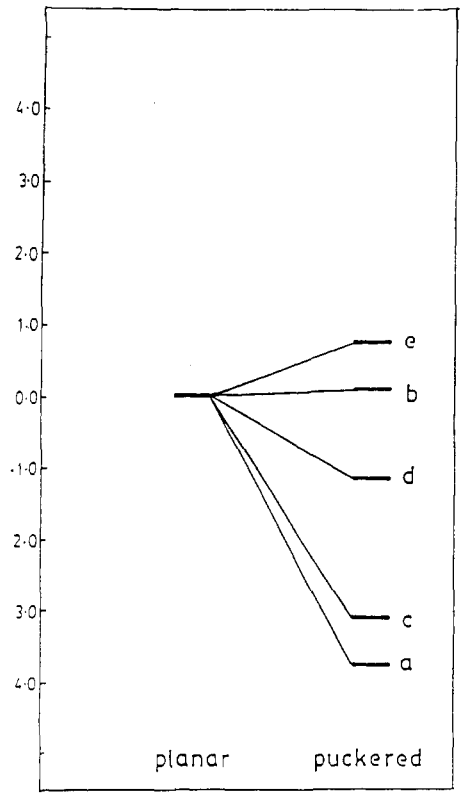

Figure 6. Sum of the one-electron energies of (a) $[CpTiP_6TiCp]$, 24 VE; (b) $[CpVP_6VCp]$, 26 VE; (c) $[CpTiAs_6TiCp]$, 24 VE; (d) $[CpTiC_6H_6TiCp]$, 24 VE; and (e) $[CpVC_6H_6VCp]^{2+}$, 24 VE, as a function of puckering of the middle ring.

the puckered than in the planar form, as the sum of the one-electron energies indicates (Figure 6). The 24-VE model complex $[CpVC_6H_6VCp]^{2+}$, however, should be more stable in the planar form for reasons that we will discuss now.

Three-Dimensional Delocalization in 24-VE Complexes. In 28-VE complexes the $1e_2'$ and $2e_2'$ orbitals, **5**, are all occupied, whereas in 24-VE systems only the $1e_2'$ bonding orbitals are occupied and the $2e_2'$ antibonding orbitals are vacant. In such a case there are two possibilities for the complex to attain stability. The first one is, as we have already explained, a puckering of the middle ring. The other one is to get stabilized by three-dimensional delocalization.

Which of the two possibilities is observed largely depends on the energy of the b_{2g} orbital of the middle ring present in the complex. P_6 and As_6 middle rings have their b_{2g} orbitals at appropriate energy to stabilize the metal–metal bonding orbital, a_1', in the puckered form, while the higher lying b_{2g} orbital of the C_6H_6 ring provides only a small stabilization. In addition to this, the aromatic stabilization of benzene is much higher than that of the P_6 ring. This makes the puckering of the C_6H_6 a much less favorable process.

In such a situation a 24-VE complex of C_6H_6 is stabilized in the planar form by three-dimensional delocalization. Only the 24-VE complex $[CpTiC_6H_6TiCp]$ should contain a puckered benzene ring. For $[CpVC_6H_6VCp]^{2+}$ we calculate a planar C_6H_6 ring structure.

The reasons are that the CpTi···TiCp orbitals have the appropriate energy to be stabilized by the b_{2g} orbital of the puckered C_6H_6 ring and the Ti orbitals are more diffuse than those of V.

This three-dimensional delocalization is well known in organic and carbaborane chemistry. Adamantane[15] and *closo*- and *nido*-carbaboranes[14,16,17] also show three-dimensional aromaticity with the appropriate number of electrons.

Conclusions

The cothermolysis of $[Cp''Nb(CO)_4]$ (**1**) and P_4 yields the 26-VE triple-decker complex $[(Cp''Nb)_2(\mu\text{-}\eta^6\text{:}\eta^6\text{-}P_6)]$ (**2**). X-ray structure determination shows that the P_6 middle deck is severely bisallylically distorted.

The two different modes of in-plane distortion observed in the 26-VE complexes of V and Nb are due to the presence of two electrons in the nearly degenerate $2e_2'$ antibonding orbitals and the occupancy of either the 5a or 5b component (Figures 2 and 5).

Twenty-four-valence-electron triple-decker complexes with P_6 and As_6 as middle rings prefer a puckered middle ring structure because of the stabilization of the metal–metal bonding orbital, a_1', and the large HOMO–LUMO gap. It is the strong antibonding character of the e_2' orbitals in the puckered form which makes the planar triple-decker structures more favorable in 26- or 28-VE complexes (Figures 3, 5, and 6).

Compared to P_6 and As_6 rings, the benzene ring is much less susceptible to puckering. This can be traced to only a weak interaction between the b_{2g} orbital of the C_6H_6 ring and the metal fragment.

In planar 24-VE triple-decker complexes, depending on the type of middle ring present, three-dimensional delocalization is observed.

Appendix

Atomic parameters for all the atoms used in the calculations were taken from previous studies.[18-21] Geometrical parameters were taken from the experimentally determined structures wherever possible. All C–C and C–H distances used in the calculations are 1.41 Å nd 1.08 Å, respectively.

Acknowledgment. We are grateful to the National Informatic Centre and the University of Hyderabad for computations. A.C.R. thanks the Council of Scientific and Industrial Research, New Delhi, and the Department of Science and Technology, New Delhi, for financial assistance. A grant of the Fonds der Chemischen Industrie for R.W. is gratefully acknowledged.

Supplementary Material Available: Tables of X-ray crystallographic data, positional and isotropic thermal parameters, anisotropic thermal parameters, and bond lengths and angles for compound **2** (8 pages). Ordering information is given on any current masthead page.

OM920335S

(14) Jemmis, E. D.; Pavankumar, P. N. V. *Proc. Indian Acad. Sci. (Chem. Sci.)* **1984**, *93*, 479.
(15) Bremer, M.; Schleyer, P. v. R.; Schötz, K.; Kausch, M.; Schindler, M. *Angew. Chem.* **1987**, *99*, 795; *Angew. Chem., Int. Ed. Engl.* **1987**, *26*, 761.
(16) Jemmis, E. D.; Schleyer, P. v. R. *J. Am. Chem. Soc.* **1982**, *104*, 4781.
(17) Jemmis, E. D. *J. Am. Chem. Soc.* **1982**, *104*, 7017.
(18) Sung, S.-S.; Hoffmann, R. *J. Am. Chem. Soc.* **1985**, *107*, 578.
(19) Hoffman, D. M.; Hoffmann, R.; Fisel, C. R. *J. Am. Chem. Soc.* **1982**, *104*, 3858.
(20) Underwood, D. J.; Nowak, M.; Hoffmann, R. *J. Am. Chem. Soc.* **1984**, *106*, 2837.
(21) Kamata, M.; Yashida, T.; Otsuka, S.; Hirotsu, K.; Higuchi, T.; Kida, M.; Tatsumi, K.; Hoffmann, R. *Organometallics* **1982**, *1*, 227.